

# The photophoretic sweeping of dust in transient protoplanetary disks

O. Krauss<sup>1</sup>, G. Wurm<sup>1</sup>, O. Mousis<sup>2</sup>, J.-M. Petit<sup>2</sup>, J. Horner<sup>3,\*</sup>, and Y. Alibert<sup>3</sup>

<sup>1</sup> Institut für Planetologie, University of Münster, Wilhelm-Klemm-Str. 10, 48149 Münster, Germany  
e-mail: okrauss@uni-muenster.de

<sup>2</sup> Observatoire de Besançon, CNRS-UMR 6091, BP 1615, 25010 Besançon Cedex, France

<sup>3</sup> Physikalisches Institut, University of Bern, Sidlerstrasse 5, 3012 Bern, Switzerland

Received 8 September 2006 / Accepted 6 November 2006

## ABSTRACT

**Context.** Protoplanetary disks start their lives with a dust free inner region where the temperatures are higher than the sublimation temperature of solids. As the star illuminates the innermost particles, which are immersed in gas at the sublimation edge, these particles are subject to a photophoretic force.

**Aims.** We examine the motion of dust particles at the inner edge of protoplanetary disks due to photophoretic drag.

**Methods.** We give a detailed treatment of the photophoretic force for particles in protoplanetary disks. The force is applied to particles at the inner edge of a protoplanetary disk and the dynamical behavior of the particles is analyzed.

**Results.** We find that, in a laminar disk, photophoretic drag increases the size of the inner hole after accretion onto the central body has become subdued. This region within the hole becomes an optically transparent zone containing gas and large dusty particles ( $\gg 10$  cm), but devoid of, or strongly depleted in, smaller dust aggregates. Photophoresis can clear the inner disk of dust out to 10 AU in less than 1 Myr. The details of this clearance depend on the size distribution of the dust. Any replenishment of the dust within the cleared region will be continuously and rapidly swept out to the edge. At late times, the edge reaches a stable equilibrium between inward drift and photophoretic outward drift, at a distance of some tens of AU. Eventually, the edge will move inwards again as the disk disperses, shifting the equilibrium position back from about 40 AU to below 30 AU in 1–2 Myr in the disk model. In a turbulent disk, diffusion can delay the clearing of a disk by photophoresis. Smaller and/or age-independent holes of radii of a few AU are also possible outcomes of turbulent diffusion counteracting photophoresis.

**Conclusions.** This outward and then inward moving edge marks a region of high dust concentration. This density enhancement, and the efficient transport of particles from close to the star to large distances away, can explain features of comets such as high measured ratios of crystalline to amorphous silicates, and has a large number of other applications.

**Key words.** stars: circumstellar matter – stars: planetary systems: protoplanetary disks – solar system: formation – comets: general

## 1. Introduction

There is virtually no doubt that planetary systems form within protoplanetary disks, which result as the dense cores of molecular clouds collapse and new stars accrete in their centre (Bouvier et al. 2006). Protoplanetary disks initially consist mostly of gas, with dust making up only  $\sim 1\%$  of the mass. The dust and gas are often considered to be coupled to each other by this typical 1% ratio. This is justified for the interstellar medium, where dust is only subject to minor size alterations. It is, however, a treacherous assumption for protoplanetary and circumstellar disks, where particles are known to rapidly evolve, leading to the formation of large structures (planetesimals) (Dominik et al. 2006; Weidenschilling 2000). Therefore, it is important to note at the very beginning of this paper that, within the scope of this work, the gas and the solids are considered to be two different components of the protoplanetary disk. In fact, we will show that they might become partially separated by the effect of photophoresis for significant time spans over the lifetime of a disk. According to current statistics detailing the detection of

extrasolar planets and disks, many protoplanetary disks leave behind planetary systems or debris disks (Greaves et al. 2006). What remains nebulous is the timing of planet, asteroid and comet formation within the lifetime of the protoplanetary disks (generally a few Myr). If the formation or shaping processes take place rather late, it is important to know how the transition from an optically thick gaseous and dusty disk to a debris disk in which most gas and dust is gone occurs. In two recent papers, Krauss & Wurm (2005) and Wurm & Krauss (2006) assumed that the dust might evolve on shorter timescales than the gas. They considered a late disk, still rich in gas, but optically thin to radiation from the star. In this case, photophoresis transports any remaining or replenished dust efficiently outwards and concentrates it in belts at several tens of AU. Petit et al. (2006) showed that in an evolving disk, the concentration radius moves inwards again. The concentration thus sweeps back and forth over the early outer Solar system (sweeping through regions such as the Kuiper belt), and changes the amount of crystalline silicates which will be added to the bodies in these regions from a source in the inner Solar system.

The existence of gaseous, yet transparent disks is supported by observations of a class of transitional protoplanetary disks

\* *Current address:* Astronomy Group, Open University, Walton Hall, Milton Keynes MK7 6AA, UK.

with large inner holes, such as TW Hya, CoKu Tau/4, DM Tau, and LkCa 15 (Calvet et al. 2002; Forrest et al. 2004; D’Alessio et al. 2005; Bergin et al. 2004; Calvet et al. 2005). Such objects make up about 10% of protoplanetary disks (Sicilia-Aguilar et al. 2006). Models imply that they have large inner holes of several AU radii (Calvet et al. 2002). These inner holes are essentially free of dust, with a sharp transition to an optically thick dusty outer disk. It certainly has to be assumed that gas is present at the inner edge of the disk, and further outwards where dust is present. However, even within the region cleared of dust, gas is obviously present as some of the objects show signs of active accretion (Najita et al. 2006; Rettig et al. 2004). The location of the sharp inner edge as a function of time can be understood by the application of photophoretic drift, as we will show in this paper. Photophoresis naturally explains the clearing of small particles from the inner few AU on rather short timescales, as soon as an inner hole of radius  $\sim 0.5$  AU (or less) is present. Photophoresis always acts on particles at the inner edge of protoplanetary disks. Initially, the radius of the inner edge from the star might be equal to the sublimation radius. As soon as accretion decreases sufficiently, photophoresis will (given certain assumptions) trigger the clearing of protoplanetary disks. The dust edge will move outwards, away from the sublimation radius. The inner edge represents a strong enhancement in solid density, and contains material which is transported over tens of AU from the inner system to the outer regions. The transportation of material in this way has a large number of applications. To warrant readability, and not overwork the manuscript, we merely highlight the applications here and will publish details separately. For clarity, this paper will remain focused on the model of the migration of the dusty edge outwards and inwards again. We present a unified model of small particle migration based on the ideas of photophoretic drift and concentration quantified in Krauss & Wurm (2005) and Petit et al. (2006). As our example protoplanetary disk, we use an  $\alpha$ -disk model (Shakura & Sunyaev 1973), taking into account the effect of photoevaporation (Papaloizou & Terquem 1999; Alibert et al. 2005a). We also introduce a more elaborate treatment of photophoresis which is applicable in all parts of protoplanetary disks and for all particle sizes smaller than 10 cm.

## 2. Photophoresis

The surface of a solid particle embedded in a gas is usually heated heterogeneously by light. Gas molecules accommodated and rejected at the surface will carry different momentum and a net force on the particle results – photophoresis (Rohatschek 1985; Ehrenhaft 1918). The effect is strongly pressure dependent. It mostly goes unnoticed at normal atmospheric pressure on Earth, but becomes strong for the pressures that are prevalent in protoplanetary disks. Krauss & Wurm (2005) and Wurm & Krauss (2006) used an approximation for photophoresis in the free molecular flow regime. For small particles ( $< 1$  mm), this is applicable in regions at radii  $> 0.5$  AU in the minimum mass solar nebula of Hayashi et al. (1985). However, the description for the denser regions further in, and for larger particles further out, requires a more detailed treatment of photophoresis. The conditions can be described best by the Knudsen number,  $Kn$ , which is defined as  $Kn = l/a$ , where  $l$  is the mean free path of the gas molecules and  $a$  is the radius of the particle in question. If the mean free path of the gas molecules is no longer large compared to the particle sizes considered, i.e. for  $Kn < 1$ , the gas flow changes from free molecular flow to the continuum regime. Under these conditions, the photophoretic force

also changes its pressure dependence from a linear *increase* with pressure in the mean free molecular flow regime to a linear *decrease* with pressure in the continuum regime. This has to be taken into account. A semi-empirical approach to a description of the photophoretic force  $F_{\text{ph}}$  for all gas pressures  $p$  has been given by Rohatschek (1995). In an alternative (and more rigorous) treatment by Beresnev et al. (1993) the photophoretic force on a spherical particle, valid for both flow regimes, is given as

$$F_{\text{ph}} = \frac{\pi}{3} a^2 I J_1 \left( \frac{\pi m_g}{2kT} \right)^{1/2} \frac{\alpha_E \psi_1}{\alpha_E + 15 \Lambda Kn (1 - \alpha_E)/4 + \alpha_E \Lambda \psi_2}, \quad (1)$$

where  $I$  is the light flux,  $m_g$  is the average mass of the gas molecules ( $3.914 \times 10^{-27}$  kg),  $T$  is the gas temperature, and  $k$  the Boltzmann constant.  $J_1$  is the asymmetry factor that contains the relevant information on the distribution of heat sources over the particle’s surface upon irradiation. In the simplest case, when the incident light is completely absorbed on the illuminated side of the particle, it is  $J_1 = 0.5$ , which we will assume in the calculations below. The energy accommodation coefficient  $\alpha_E$  is the fraction of incident gas molecules that accommodate to the local temperature on the particle surface and, thus, contribute to the photophoretic effect. In the following, we assume complete accommodation, i.e.  $\alpha_E = 1$ . The corresponding coefficients,  $\alpha_n$  and  $\alpha_\tau$ , for the normal and tangential momentum accommodation, respectively (Beresnev et al. 1993), are already assumed to be 1, when expressing  $F_{\text{ph}}$  by Eq. (1). The thermal relaxation properties of the particle are summarized in the heat exchange parameter  $\Lambda = \lambda_{\text{eff}}/\lambda_g$ , where  $\lambda_g$  is the thermal conductivity of the gas and  $\lambda_{\text{eff}}$  the effective thermal conductivity of the particle. This term includes the conduction of heat through the particle, and the thermal emission from the particle’s surface, according to

$$\lambda_{\text{eff}} = \lambda_p + 4\epsilon\sigma T^3 a. \quad (2)$$

Here,  $\lambda_p$  is the thermal conductivity of the particle,  $\epsilon$  is the emissivity which we assume to be 1 further on, and  $\sigma$  is the Stefan-Boltzmann constant. The functions  $\psi_1$  and  $\psi_2$  in Eq. (1) depend only on  $Kn$  in the form

$$\psi_1 = \frac{Kn}{Kn + (5\pi/18)} \left( 1 + \frac{2\pi^{1/2} Kn}{5Kn^2 + \pi^{1/2} Kn + \pi/4} \right),$$

$$\psi_2 = \left( \frac{1}{2} + \frac{15}{4} Kn \right) \left( 1 - \frac{1.21\pi^{1/2} Kn}{100Kn^2 + \pi/4} \right). \quad (3)$$

It should be noted that an additional photophoretic force arises if the accommodation coefficients vary over the surface of the dust grain (Cheremisin et al. 2005), but we restrict the treatment to the classical photophoretic force as given in Eq. (1). To summarize, Eq. (1) is valid for all parts of protoplanetary disks and all particles, and in the following we assume  $J_1 = 0.5$ ,  $\alpha_E = 1$ , and  $\epsilon = 1$ .

## 3. The disk model

In this paper, we use a rather simple model for the solar nebula, namely an  $\alpha$  1+1D turbulent model. We provide a brief description here, but more details can be found in Alibert et al. (2005a), and Papaloizou & Terquem (1999).

In the  $\alpha$ -disk model, the radial evolution of the nebula is governed by the following diffusion equation, modified to take photo-evaporation into account:

$$\frac{d\Sigma}{dt} = \frac{3}{r} \frac{\partial}{\partial r} \left[ r^{1/2} \frac{\partial}{\partial r} \nu \Sigma r^{1/2} \right] + \dot{\Sigma}_w(r), \quad (4)$$

where  $\Sigma$  is the surface density of mass in the gas phase in the nebula,  $r$  is the distance to the Sun, and  $\nu$  the mean (vertically averaged) viscosity. The photo-evaporation term,  $\dot{\Sigma}_w(r)$ , is taken to be the same as in Veras & Armitage (2004). The mean viscosity is determined from the calculation of the vertical structure of the nebula: for each radius,  $r$ , the vertical structure is calculated by solving the equation for hydrostatic equilibrium, together with the energy equation (which states that the dissipation of energy by viscosity is balanced by the removal of energy by diffusion), and the diffusion equation for the radiative flux. The local viscosity (as opposed to that averaged in the vertical direction) is calculated using the standard Shakura & Sunyaev (1973)  $\alpha$ -parametrization  $\nu = \alpha C_s^2 / \Omega$ , where the local speed of sound,  $C_s$ , is determined by the equation of state, and  $\Omega^2 = GM_\odot / r^3$ . Using this procedure, we calculate, for each radius,  $r$ , from the Sun, and for each value of the surface density, the distribution of pressure, temperature and density. We then derive the mid plane pressure and temperature, as well as the mean viscosity inside the disk. These quantities are finally used to solve the diffusion equation (Eq. (4)), and to calculate the pressure- and temperature-dependent forces on dust grains as outlined in Sect. 4.

The structure of the nebula depends on two physical quantities, namely the equation of state, and the opacity law. For the equation of state, we use that developed by Saumon et al. (1995), taking the fraction of helium to equal 0.24. The opacity law used in our model is taken from Bell & Lin (1994) at low temperatures, and Alexander & Ferguson (1994) at higher temperatures. At low temperatures, the opacity law takes into account the contributions from different types of grains, as well as their sublimation, depending on the local temperature. Note, however, that by modifying the local abundance of dust grains inside the nebula, photophoresis may change the opacity, and therefore the structure of the nebula itself. This retroaction is not taken into account in our model, and will be the subject of future work.

Some initial parameters have to be specified in order to calculate the evolution of the solar nebula. We assume that the gas surface density is initially given by a power law  $\Sigma \propto r^{-3/2}$ , with an initial value taken to be  $\Sigma(5.2 \text{ AU}) = 600 \text{ g/cm}^2$ . The mass of the nebula (between 0.25 AU and 30 AU) is  $\sim 0.05 M_\odot$ . The photo-evaporation rate is taken as being equal to  $\sim 1.5 \times 10^{-8} M_\odot/\text{yr}$ , leading to a nebula lifetime of the order of  $\sim 3 \text{ Myr}$ . These values were used by Alibert et al. (2005c) to calculate formation models of Jupiter and Saturn consistent with the internal structure and atmospheric compositions of these two planets. For the viscous parameter, we set  $\alpha = 0.002$ . The radial dependence of the resulting surface density at different ages of the disk is shown in Fig. 1.

#### 4. Outward and inward drifts

In a protoplanetary disk where the gas pressure (in the mid plane) decreases with distance from the star, the gas is supported by a pressure gradient, and rotates slower than the Keplerian velocity (Weidenschilling 1977). Solid particles are only stable on a Keplerian orbit. Therefore, interaction with the gas leads to an inward drift of solids toward the star. For particles which couple to the gas flow on timescales small compared to an orbital period, the problem can be treated as being radial. The inward drift is then induced by the fraction of gravity (residual gravity) which is not balanced by the circular motion with the sub-Keplerian gas

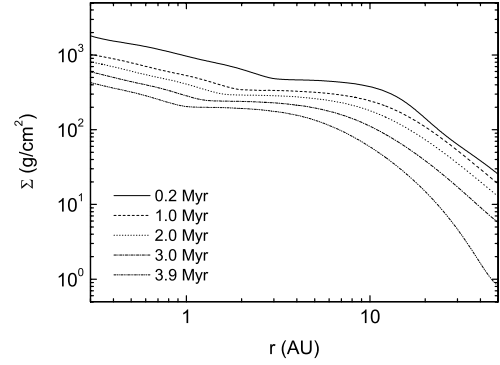


**Fig. 1.** The temporal evolution of the surface density of mass in the gas phase as a function of the distance from the star.

velocity. The force,  $F_{\text{res}}$ , acting on a particle of mass  $m_p$  due to residual gravity is given as

$$F_{\text{res}} = \frac{m_p}{\rho_g} \frac{dp}{dr}. \quad (5)$$

Here,  $\rho_g$  is the density and  $p$  the pressure of the gas.

In addition, for small particles, radiation pressure also has to be considered. Since we already assumed perfect absorption of particles, we neglect the contribution to radiation pressure from scattering, and obtain the following expression for the radiation pressure force

$$F_{\text{rad}} = \pi a^2 \frac{I}{c_{\text{light}}}, \quad (6)$$

with  $c_{\text{light}}$  being the speed of light. The sum of the outward forces (Eqs. (1) and (6)) and the inward force (Eq. (5)) is the drift force  $F_{\text{drift}}$ . We treat the problem as being purely radial here, since we are mostly interested in the small particles. These small particles couple to the gas on timescales much smaller than the orbital timescale, which justifies the radial treatment as outlined in Wurm & Krauss (2006). We estimate the radial drift velocity to be

$$v_{\text{dr}} = \frac{F_{\text{ph}} + F_{\text{rad}} + F_{\text{res}}}{m_p} \tau, \quad (7)$$

where  $\tau$  is the gas grain coupling time. This section considers a purely laminar disk, for which the drift of the particles with respect to the gas is adequately described by Eq. (7). In the case of a turbulent disk, this is just the average drift velocity, and turbulent diffusion must also be considered. This will be treated in Sect. 4.2.

As larger dust aggregates drift outwards they pass from a region where the continuum flow regime is valid to a region where the free molecular flow regime applies. Therefore, as with the photophoretic force, we have to consider an equation describing the gas grain friction time in both regimes. It is

$$\tau = \frac{m_p}{6\pi\eta a} C_c, \quad (8)$$

with  $\eta$  being the dynamic viscosity of the gas. This assumes Stokes friction, which is justified as the Reynolds numbers for the drift of particles smaller than 10 cm are well below 1. The Cunningham correction factor,  $C_c$ , accounts for the transition between the different flow regimes (Cunningham 1910) and is given as (Hutchins 1995)

$$C_c = 1 + Kn \left( 1.231 + 0.47e^{-1.178/Kn} \right). \quad (9)$$

For the calculation of  $Kn$  in Eqs. (3) and (9) we use the expression

$$l = \frac{2\eta}{\rho_g c} \quad (10)$$

for the mean free path,  $l$ , of the gas molecules (Beresnev et al. 1993), where  $c$  is the mean thermal velocity of the gas molecules. For large Knudsen numbers, the combination of Eqs. (8)–(10) yields

$$\tau_{\text{Ep}} = \varepsilon \frac{m_p}{\sigma_p \rho_g c}, \quad (11)$$

where  $\sigma_p$  is the geometrical cross section of the dust particle. This expression corresponds to the stopping time in the Epstein friction regime as given by Blum et al. (1996). The empirical parameter  $\varepsilon$  has a value of  $0.68 \pm 0.10$ .

The dynamic viscosity  $\eta$  is directly related to the square root of the gas temperature,  $T$ . Thus,

$$\eta = \eta_0 \sqrt{T/T_0} \quad (12)$$

with  $\eta_0 = 8.4 \times 10^{-6}$  Pas at  $T_0 = 280$  K.

For the calculations, we assume the bulk density of the dust particles to be  $\rho_p = 1 \text{ g/cm}^3$ , which is a reasonable value for dust aggregates. For the thermal conductivity of the dust particles, we take  $\lambda_p = 0.01 \text{ W/mK}$ . This can also be taken as a reasonable assumption for dust aggregates (Presley & Christensen 1997), but might be subject to debate in the future. In addition, any differences in the properties of these particles might result in some subtle selection effects. For the thermal conductivity of the gas,  $\lambda_g$ , we adopt values for molecular hydrogen for temperatures above 150 K (as tabulated by Incropera & DeWitt 2002). For smaller temperatures, helium has a larger thermal conductivity than hydrogen. With a significant fraction of the gas being helium, we assume that this helium will then determine the thermal conductivity of the gas. We use values for helium taken from the compilation of Bich et al. (1990). The radial variation of the drift velocity according to Eq. (7) is plotted in Fig. 2 for various particle sizes. This shows how particles would drift in a transparent model. The values are only to be taken as valid for particles in the inner cleared region, out to the optically thick edge of the disk.

Positive values of  $v_{\text{dr}}$  correspond to an outward drift, while negative values denote an inward drift (not plotted on this logarithmic plot). It should be pointed out that these drift velocities are with respect to the radial motion of the gas. The resulting velocities with respect to the central star might turn out to be negative, even for positive values of  $v_{\text{dr}}$ , when the inward gas motion due to stellar accretion is taken into account. This will be considered in Sect. 5 for the temporal evolution of the dust distribution. The first thing to note is that points of equilibrium occur where the drift vanishes. Stable equilibrium points where particles become concentrated are described in Krauss & Wurm (2005) and Wurm & Krauss (2006). In the disk model used here, at a time of 0.2 Myr, these stable points can be found at a distance of 40 AU for particles larger than 1 mm. Particles are eventually pushed outwards to this concentration distance. Particles smaller than about  $10 \mu\text{m}$  are pushed further outwards due to radiation pressure. However, photophoresis has two branches. If the mean free path of the gas molecules is smaller than the particle size, the photophoretic force decreases with pressure. This is responsible for a second equilibrium, which lies closer to the star for somewhat larger particles. This is seen in Fig. 2 for

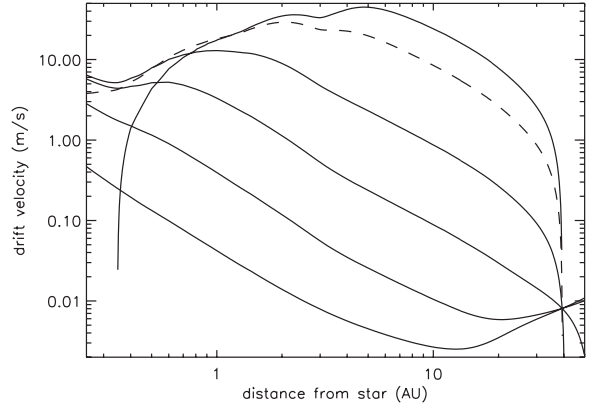


**Fig. 2.** Outward drift velocity of particles as a function of the radial distance from the star, if a disk of age 0.2 Myr were completely transparent. The curves represent particles of different sizes. *From bottom to top*, the solid curves denote particles of  $a = 1, 10, 100 \mu\text{m}$ , and  $a = 1 \text{ mm}$ . The dashed lines are for particles of  $a = 1 \text{ cm}$  and  $a = 3 \text{ cm}$ . The value for 3 cm particles turns negative inside approximately 0.4 AU. For particles larger than 1 mm the drift velocity also becomes negative beyond 40 AU.

3 cm particles which drift inwards closer than  $\approx 0.4$  AU from the star. This is not a stable equilibrium, and the particles eventually move to one side or the other of this point. Nevertheless, particles might stay in this region for a prolonged time, long enough to be subject to other processes, such as collisions with planetesimals. For larger particles, the location of the maximum drift velocity shifts to larger distances from the star. For moderate sizes, from micrometer up to a few cm, the magnitude of the drift velocity increases with particle size everywhere in the disk. Therefore, the important point is that the slowest moving particles are usually the smallest. For objects larger than about 1 m, the radial treatment would no longer hold since the gas grain friction times become comparable to the orbital period. Also, rotation becomes important for such large bodies, which will change the photophoretic force. We therefore restrict our results to particles smaller than about 10 cm, which we will call dust.

Starting with a disk which has a transparent inner region and an opaque outer region, dust particles at the inner edge are subject to photophoresis. Large particles move faster than small particles. Therefore, they are rapidly moving outwards. The slower, smaller particles remain behind and the larger particles are soon shielded from starlight. Therefore, the edge moves outwards with a drift velocity determined by the smallest particles that are able to render the disk optically thick. As the larger particles react swiftly, the edge is rather sharp, as observed for the transient disks mentioned above.

#### 4.1. Accretion due to viscous evolution

It has to be remembered that, in addition to the relative motion between solids and gas we must also consider the absolute motion of the gas. As the disk evolves viscously, it accretes onto the star with an accretion speed  $v_{\text{ac}}$ . Since the accretion speed depends on the evolutionary stage of the disk (in other words, on the elapsed time), it can act to delay the outward motion of the dust particles and then, for a short period, act to slow it down. For the young disk in the model considered here, the accretion speed at 1 AU is about  $20 \text{ cm s}^{-1}$ , dropping to  $1 \text{ cm s}^{-1}$  beyond 10 AU. At later times, the inner value drops to a few  $\text{cm s}^{-1}$  while the value at larger distances changes little.

As can be seen in Fig. 2, the accretion is comparable to the outward drift for  $1\ \mu\text{m}$  particles with an assumed thermal conductivity of  $\lambda_p = 0.01\ \text{W m}^{-1}\ \text{K}^{-1}$ , but as soon as the particles reach  $10\ \mu\text{m}$  or larger, or if they have a lower thermal conductivity, accretion ceases to be an obstacle to outward drift.

#### 4.2. Turbulent diffusion

In a turbulent disk, a fraction of the particles experience a faster or slower inward drift due to turbulent diffusion. This acts to shift the transition region between the optically thick outer disk and the optically thin inner region further inwards. If this is more effective than photophoresis, no outward drift of the inner edge will occur. If the inner edge drifts inwards more slowly than it moves outwards due to photophoresis, then diffusion will not completely stop the outward motion, but will slow down or change the characteristics of the clearing of solids from the disk.

The fraction of diffusing particles that is necessary to move the transition between transparent and opaque disk inwards depends on the particle sizes and number densities present at a given time and location, together with their diffusion speeds. A detailed treatment of turbulent diffusion working together with photophoretic drift is beyond the scope of this paper and will be addressed in detail in future studies. However, some reasonable and some extreme estimates for turbulent diffusion are given here to illustrate the effect of turbulence on the photophoretic evolution of a disk. The case in which diffusive drift is underestimated to the greatest extent has already been given by the laminar case, which assumes that a particle which is picked up by a turbulent eddy and is transported inwards will be transported outwards again by the same eddy, which will return it to its original position. No net drift would result. An extreme overestimation is the case where particles are handed inwards from one of the large eddies to another large eddy, and so on, with a resulting maximum speed of the turbulent gas of more than  $100\ \text{m s}^{-1}$  (Supulver & Lin 2000; Dullemond & Dominik 2004). If that were the case for a large fraction of particles photophoresis would not be able to clear an optically thick disk at all as photophoretic drift velocities are, in general, smaller than  $100\ \text{m s}^{-1}$ . However, turbulence can be described as a cascade of eddies of different size, and inward as well as outward motions occur as a particle adapts to the changing gaseous environment. Therefore, the effective diffusion speed is somewhere between the extreme cases. This kind of random walk in a turbulent cascade has already been studied (for example, by Supulver & Lin 2000).

For simplicity, we assume here that turbulent diffusion does not depend on the particle size for the range of particle sizes considered ( $<10\ \text{cm}$ ), and that inward diffusion is described by a constant velocity,  $v_{\text{turb}}$ . Certainly, in general, this is misleading as diffusion cannot be defined as a velocity. Diffusion is typically characterized by the distance travelled by a particle as a function of the square root of time. However, keeping that in mind, it suffices for estimating the possible effects in this case.

Realistic values of a turbulent diffusive drift should be significantly larger than the laminar case ( $v_{\text{turb}} = 0\ \text{m s}^{-1}$ ), but also much smaller than the extreme ( $v_{\text{turb}} \ll 100\ \text{m s}^{-1}$ ). Detailed particle tracks in a turbulent disk are given in the Monte Carlo simulations by Supulver & Lin (2000). One of their important results is that 85% of  $5\ \text{mm}$  particles placed between 2 and 3 AU move outwards rather than inwards. However, the detailed track of a  $1\ \text{cm}$  particle shows numerous parts of its trajectory where it moves inwards with a maximum speed of about  $5\ \text{m s}^{-1}$  (estimated from their Fig. 8b). Supulver & Lin (2000) assume

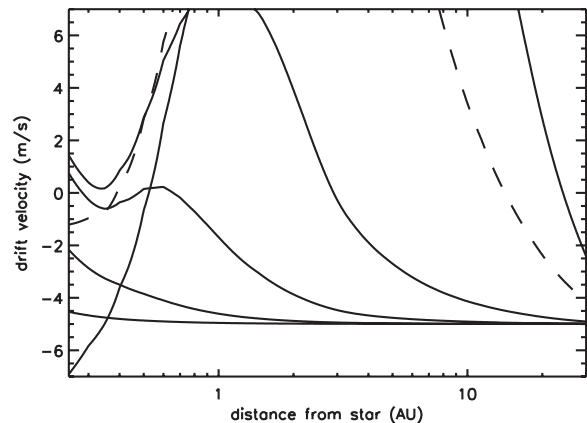


**Fig. 3.** Particle drift and turbulent diffusion at 0.2 Myr. As in Fig. 2 from bottom to top, the solid curves denote particles of  $a = 1, 10, 100\ \mu\text{m}$ , and  $a = 1\ \text{cm}$  and  $a = 3\ \text{cm}$ , respectively. A constant turbulent inward diffusion of  $5\ \text{m s}^{-1}$  has been subtracted for all particle sizes.

a viscous parameter  $\alpha = 10^{-2}$ , which is comparable to the value of  $\alpha = 0.002$  assumed in our model. Therefore, a maximum turbulent diffusion drift for the optically thick edge in our model might be estimated as  $v_{\text{turb}} = 5\ \text{m s}^{-1}$ . It should be noted that photophoretic drift is counteracted by a much smaller diffusive drift if the fast diffusing particles are not numerous enough to increase the opacity of the disk. More realistic values might therefore be much smaller than  $5\ \text{m s}^{-1}$ , but a detailed treatment is postponed to future studies of diffusion at the inner edge. In any case, diffusion will slow down the photophoretic motion of particles. Figure 3 illustrates what effect diffusion imposes on particles of different size. The drift velocities according to Eq. (7) are used, but a constant diffusive drift of  $5\ \text{m s}^{-1}$  is subtracted. In a disk (stage) that has an opaque outer region and that is dominated by particles with negative drift values, no outward drift is possible. In our model, this is the case if the turbulent disk is dominated by particles smaller than  $100\ \mu\text{m}$ . This result is not very sensitive to the exact value of the diffusion speed of  $5\ \text{m s}^{-1}$ . As small particles already drift rather slowly in the laminar case, the diffusion speed has to be a factor of 10 smaller before being considered negligible. The existence of a sufficient fraction of particles smaller than  $100\ \mu\text{m}$  might therefore offset any clearing of the disk until either the turbulence subdues significantly or the small particles vanish (through, for example, coagulation).

In addition to these considerations, cm-sized particles cannot move away from a close inner rim (at about 0.5 AU or less) at early times as the photophoretic force acting on them is weak due to the small Knudsen numbers. An initial early clearing is only possible if a monodisperse size distribution of particles somewhat smaller than 1 mm exists. Once a gap of 0.5 AU is formed (one way or the other), or if the gas density in the inner region decreases, cm-size particles can also be pushed further out. It is interesting to note that in a turbulent disk consisting of mm-sized dust particles, the inner edge might not move further out than a few AU (3 AU with the given parameters). The position of the inner edge will then be almost constant even as the disk evolves and the gas density decreases, which will be shown in Sect. 5.2.

In a laminar transparent disk, particles become concentrated at more or less the same distance (several tens of AU) independent of their size. Caution should be used when comparing this scenario with the particle size-dependent position of the inner

edge. The same size-independent concentrations at large distances will also occur in a turbulent disk if the disk is completely transparent. The position of the edge is merely smeared out by turbulence but is not shifted by diffusion. A size-dependent position of the inner edge requires the outer disk to be opaque so that particles can be illuminated or shadowed.

## 5. Temporal evolution of the dusty edge

In the model of photophoretic clearing discussed here, the smallest particle size is the critical parameter. Unfortunately, little can be said, in general, about the evolution of the size of the smallest particles abundant enough to make the disk optically thick.

In simple growth models that only consider sticking of particles in collisions, the growth is incredibly quick. Particles will grow to cm-size in a few thousand years (Dominik et al. 2006; Weidenschilling 2000). This simple growth mechanism to cm-size is in full agreement with experimental findings (Blum et al. 2000; Blum & Wurm 2000). However, as soon as particles grow further, collisions will start to produce a new population of smaller particles. Recent experiments show that the growth of a larger body and the generation of smaller fragments of dusty bodies can occur in the same collision (Wurm et al. 2005). This will replenish the reservoir of small particles but, unfortunately, there is currently no realistic prediction for the size distribution of small particles resulting from fragmentation and growth, and, due to the lack of more reliable data, we will assume (somewhat arbitrarily) an exponential evolution here,

$$a = a_0 e^{t/t_0} \quad (13)$$

with  $a_0$  and  $t_0$  being free parameters. It is plausible that, as larger bodies form and the amount of matter redistributed to the dust component gets smaller, growth by coagulation will dominate, and the smallest particle size will shift to larger values. Otherwise, the details might be responsible for the differences in the evolution of different systems (for example, the position of the inner dust edge at different distances for stars of similar ages). Once the minimum particle size has reached a value of 1 cm, we turn the temporal evolution of particle size off. Thereafter, we calculate particle drifts assuming a constant size of 1 cm. This accounts for the fact that, for reasonable nebula masses, particles larger than this cease to have a significant effect on the opacity of the disk. It is also tied into the fact that our treatment of photophoresis only applies to particles smaller than 10 cm. Particles of cm-size move so rapidly that they essentially trace the position of their equilibrium point where all radial forces are balanced. This equilibrium exists for particles larger than 1 mm and its position is independent of particle size (see Fig. 2). Therefore, the cm-sized particles effectively trace the position within the disk where the small particles that now make up an optically thin fraction of the disk will become concentrated. These particles represent a combination of replenished material and the remains of the initial dust population, and are between 1 mm and 10 cm in size.

### 5.1. Particle motion in a laminar disk

With the assumptions and disk model given above, we investigate the motion of the edge due to the effect of photophoresis acting on the smallest particles. Therefore, the position of the

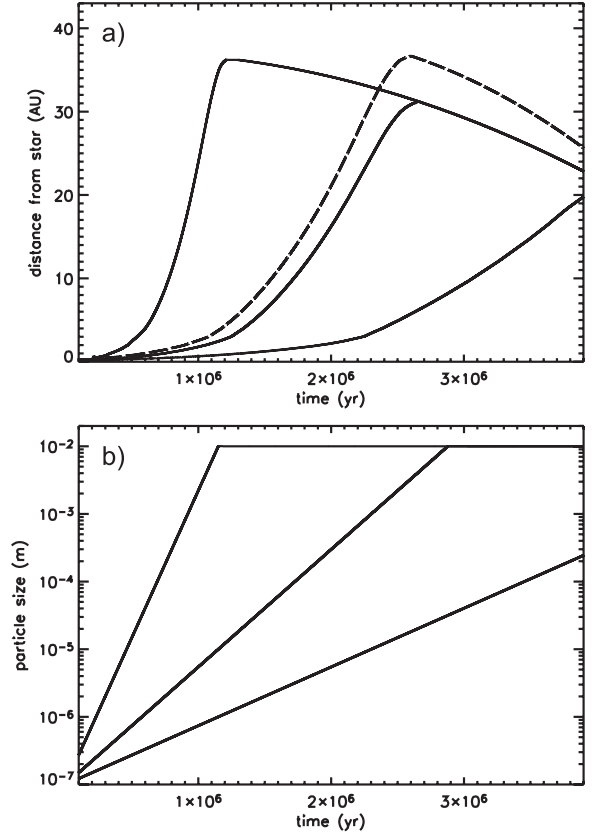


**Fig. 4.** **a)** The position of the inner edge of the dust disk as a function of time for different particle growth timescales. For the solid lines, the growth timescale is  $t_0 = 100\,000$  yr,  $t_0 = 250\,000$  yr, and  $t_0 = 500\,000$  yr (moving from left to right), and  $\lambda_p = 0.01\text{ W m}^{-1}\text{ K}^{-1}$ . The dashed line is for  $t_0 = 250\,000$  yr and  $\lambda_p = 0.005\text{ W m}^{-1}\text{ K}^{-1}$ . The evolution is divided into 3 parts. With increasing time, these parts correspond to slow drift, fast drift, and an inward retreat. **b)** Corresponding particle size evolution. The growth is cut-off once the particles have reached a size of 1 cm. Comparison with **a)** shows that the edge only starts to move outwards efficiently once particles have grown to  $10\ \mu\text{m}$  or larger.

edge,  $R(t_{\text{disk}})$ , at the age of the disk,  $t_{\text{disk}}$ , is calculated by numerically solving

$$R(t_{\text{disk}}) = \int_0^{t_{\text{disk}}} (v_{\text{dr}}(a(t), R(t)) - v_{\text{ac}}(R(t))) dt. \quad (14)$$

It has to be noted that the assumptions above do not consider the diffusion of particles due to turbulence (as discussed in Sect. 4.2). Only the average particle motion due to the viscous evolution of the disk is taken into account by including  $v_{\text{ac}}$ . As outlined above, a fraction of particles which diffuse inwards faster than average due to turbulent diffusion has the potential of rendering the disk optically thick. We discuss the possible effects of turbulent particle transport on the evolution of the inner edge in Sect. 5.2.

We start with particles placed at the inner edge of the model disk, at 0.25 AU, which is in good agreement with the initial sublimation distance since the temperature is much larger than 1000 K at this location in our model disk. We assume that the particles are initially of interstellar size ( $a_0 = 0.1\ \mu\text{m}$ ). As our timescales for growth, we take  $t_0 = 100\,000$  yr,  $t_0 = 250\,000$  yr, and  $t_0 = 500\,000$  yr. We also calculate the evolution of particles with a growth timescale of  $t_0 = 250\,000$  yr, but a lower thermal conductivity of  $\lambda_p = 0.005\text{ W m}^{-1}\text{ K}^{-1}$ . The evolution of the position of the inner disk edge for these four scenarios is shown

in Fig. 4a. The underlying growth of the particles is depicted in Fig. 4b. As can be seen, the edge starts to move outwards after a few 100 kyr, as the accretion becomes slow enough, and the particles grow sufficiently to move more rapidly.

The evolution of the dusty edge can be divided into three discrete phases. For the first few 100 kyr, the edge does not move at all, or only moves very slowly due to the combination of the high accretion rate and the small particle sizes. As can be seen in Fig. 4b, this corresponds to a period when the particles are smaller than  $10\ \mu\text{m}$ . Once the particles have grown beyond that size, the dusty edge moves outwards. When the particles have grown larger than about  $1\ \text{mm}$  they rapidly move to the equilibrium position, where all drift forces are balanced. As growth proceeds over time, it is likely that the overall dust density at the edge, and in the optically thick outer part, decreases strongly with time. In fact, as our model assumes growth of the particles, it is conceivable that the whole disk might turn optically thin before it reaches the end of its viscous evolution. In this case, the edge at later times would no longer be an inner edge but rather a concentration of the remaining or replenished particles in a ring-like distribution, as described in Krauss & Wurm (2005) and Petit et al. (2006). As the gas density in the disk decreases over time, the photophoretic force on the dust grains gets weaker, and the equilibrium position moves inward again leading to a dust ring with decreasing radius (Petit et al. 2006). The length of the three evolutionary phases is obviously directly connected to the time constant of the particle growth process. The faster the particles grow, the earlier the edge starts to move outward and reaches its maximum distance from the star. Furthermore, the maximum radius that is reached by the edge or the ring depends on how fast the dust particles grow (and also on the thermal conductivity of the grains).

## 5.2. Particle motion in a turbulent disk

The same calculations as those described in the previous subsection are carried out assuming that turbulent diffusion would counteract the photophoretic outward drift by a constant offset of  $5\ \text{m s}^{-1}$ . The resulting radial velocities are shown in Fig. 5 with the corresponding scenarios for the particle size evolution being the same as in Fig. 4b. As discussed in Sect. 4.2, small particles cannot oppose turbulent diffusion. Particles have to grow larger than  $100\ \mu\text{m}$  for photophoresis to start clearing the disk. As a consequence of this, the initiation of the outward drift of the edge is delayed longer than in the case of a non-turbulent disk. Nevertheless, the first two phases of the disk evolution are qualitatively similar to the laminar case, since the photophoretic drift of small particles is very slow and does not contribute significantly to the clearing process. However, the maximum distance achieved from the star and the behaviour during the third evolutionary phase, which is characterised by an inward motion of the edge in the laminar case, are considerably different in a turbulent disk. Due to the additional inward velocity ( $v_{\text{turb}}$ ) the edge reaches a maximum radius of only about 15 AU for  $\lambda_p = 0.01\ \text{W m}^{-1}\ \text{K}^{-1}$  and 20 AU for  $\lambda_p = 0.005\ \text{W m}^{-1}\ \text{K}^{-1}$ . Once the edge has reached this maximum distance it stays there, and barely moves while the gas is dispersed. This is a result of the fact that, if the photophoretic drift relative to the gas dominates the particle motion, the drift velocity is almost independent of the absolute gas density (Wurm & Krauss 2006). For the assumed value of turbulent diffusion, the net drift velocity equals the outward drift velocity when it is solely dominated by the photophoretic term, and is not affected by residual gravity. This is in contrast to the gas density dependent position where all drift

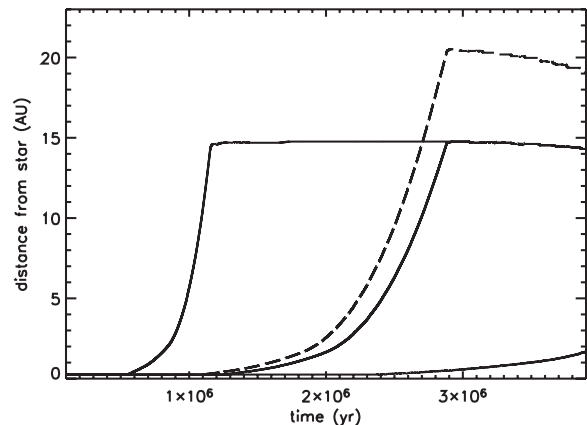


**Fig. 5.** Same as Fig. 4a but assuming  $5\ \text{m s}^{-1}$  offset due to turbulent diffusion.

forces are equal. Thus, the disk evolution has little influence on the position of the inner edge until the edge approaches the location of its inward moving laminar counterpart.

For the largest particles (cm-sized), however, the offset of  $5\ \text{m s}^{-1}$  might not be justified if the bulk of the disk is already transparent. In that case, turbulent diffusion would only smear out the distribution around the stable position of the concentration points given by the laminar case. This is, in a general sense, true for any transparent disk. Even small particles are then concentrated at their equilibrium distance as determined for the laminar case since turbulence no longer has the ability to move particles from the illuminated region into the shadow.

The turbulent offset leads to a dependence of the equilibrium position of the inner edge on particle size. If we do not cut off the particle size at  $a = 1\ \text{cm}$ , but at different sizes, the position of the inner edge shifts. In equilibrium, the inner edge is where the drift velocities turn negative in Fig. 3. These positions are plotted in Fig. 6 as a function of the particle size at a disk age of 0.2 Myr (solid line) and 3.4 Myr (dashed line). The dependence on the particle size is obvious. It can also be seen that the position of the edge changes very little during more than 3 Myr of disk evolution (for a given particle size). For particle sizes  $< 1\ \text{cm}$  it is shifted slightly outward, whereas for larger particles it moves slightly inwards.

Therefore, the qualitative differences between the laminar and the turbulent cases can be summarised as follows. When turbulent diffusion is active, the clearing of the inner disk begins later, the inner edge does not move as far out, and the position of the edge depends much more on the size evolution of the particles than on the dispersion of the gas component of the disk.

## 6. Possible applications

The evolution of disk material described in this work lends itself to a number of possible applications. A detailed discussion of these is beyond the scope of this paper, and will be carried out in a later work. However, a few simple examples serve to highlight the ideas and predictions which could be based upon photophoretic disk clearance.

In our model, the motion of the inner edge of the disk over time in the laminar case is strongly dependent on the assumptions made about the evolution of the dust particles. A different growth rate to that assumed in Eq. (13) can lead to significant changes in each of the three regions described above, either leading to an initial enhancement in the clearing rate, or acting to

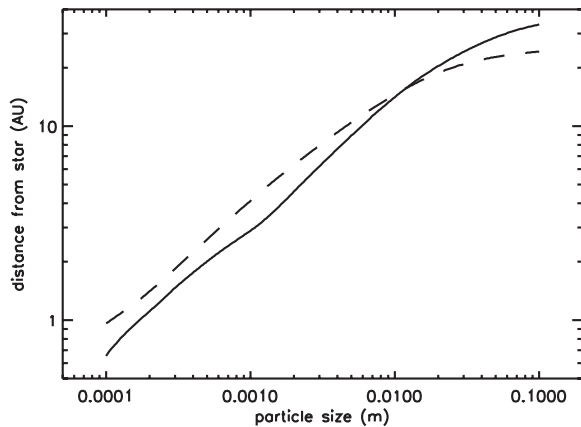


**Fig. 6.** Equilibrium position as a function of the minimum particle size for a turbulent disk at the age of 0.2 Myr (solid line) and 3.4 Myr (dashed line).

prevent the formation of a larger hole, if the disk disperses more rapidly than the smallest particles evolve. Such a wide range of possible outcomes is in close agreement with the diversity of transient disks found (Calvet et al. 2002; Forrest et al. 2004; D’Alessio et al. 2005; Bergin et al. 2004). If turbulent diffusion is important, the size of the inner hole of transient disks might be determined by the cut-off particle size rather than the growth rate and, therefore, be less dependent on time.

The formation of dust rings (Krauss & Wurm 2005; Petit et al. 2006) around youthful stars can be well explained using this model. These systems can be taken as representing old disks, nearing the end of their photophoretic evolution. If dust particles grow in such a system, this will lead to all the material eventually being devoured, and the rings will no longer be dominated by dust that evolved at the very location of the edge/ring. Dust fragments which are produced at smaller radii than the ring location (such as those created in collisions, Wurm et al. 2005; or coming from eolian erosion, Paraskov et al. 2006) would be pushed rapidly outward, and would represent a significant contribution to the ongoing survival of the ring. The equilibrium positions might thus become more and more dominated by processed dust from the inner regions. As the material concentrates in the regions where comets were supposedly formed (see Horner et al. 2006, for a discussion of the different plausible formation regions for cometary bodies), this might prove to be an important mechanism in explaining the abundance of unexpected material within these comets, such as the presence of crystalline silicates or high temperature minerals which have been detected in different objects (Campins & Ryan 1989; Bouwman et al. 2003; Sitko et al. 2004).

The timing of the formation and motion of the ring when compared to the formation and ejection epochs of the comets would definitely be an area of interest. Depending on the formation model accepted for the Oort cloud and Edgeworth-Kuiper belt, it is possible that the photophoretic dust loading would lead to observable differences between objects which reside in different reservoirs (for example, one might expect the bulk of comets that have resided in the Edgeworth-Kuiper belt to have experienced significant dust loading, while objects ejected into the Oort cloud may have escaped prior to the passage of the ring, leading to a much lower concentration of dust and high-temperature materials). Even at the most basic level, it may be that the least dusty comets represent those that were ejected to the Oort cloud at the earliest epoch, before the dusty edge had time to sweep their formation region.

As the edge moves outward and collects particles smaller than a few cm in size, it creates a region with a strong density enhancement. It is very likely that the edge could act as a trigger or boost of planetesimal formation, either by gravitational instabilities or through the mantling of preexisting planetesimal cores with an enhanced flux of small particles.

The case of the regular and irregular satellites of the gas and ice giant planets represents another possible application for this model. The regular satellites of these planets most likely formed along with the planets themselves (Alibert et al. 2005d), from the same material at the same time. The irregular satellites, by contrast, likely represent a population of captured bodies which formed elsewhere in the Solar system (Čuk & Gladman 2006; Jewitt & Sheppard 2005). It is therefore plausible that the irregular satellites may contain significantly different concentrations of dust and high-temperature materials when compared with the regular satellite families.

Some authors (Ida et al. 2000) have suggested that the Solar nebula was truncated by the passage of a nearby star during the later stages of planet formation. Such a mechanism has been invoked to explain the apparent sharp outer edge of the Edgeworth-Kuiper belt, and the presence of Sedna-like objects (Kenyon & Bromley 2004). If such an encounter did occur, it is quite possible that it could have affected the concentration of dust (which in the late stages of planet formation would be expected to be at  $\sim 30$  or 40 AU), perhaps even helping to strip this material from our Solar system entirely, aiding the truncation and diminution of the disk itself.

Finally, it is even possible that the enhanced density present in the outward-moving ring would help enhance the rates of chemical reactions in the solar nebula, through the increased concentration of catalytic material. Such enhanced reaction rates could play an important role in modifying the chemistry of the region in which the giant planets formed. In particular, the supply of high temperature material (in the form of iron or nickel grains) may ease the conversion of CO into CH<sub>4</sub> in the outer solar nebula via Fischer-Tropsch catalysis ( $\text{CO} + 3\text{H}_2 \rightleftharpoons \text{CH}_4 + \text{H}_2\text{O}$ ), since the efficiency of this reaction increases with the growing concentration of metal particles (Sekine et al. 2005). The production of CH<sub>4</sub> in the outer solar nebula in this manner has already been discussed in the literature (Prinn & Fegley 1989; Kress & Tielens 2001), but the overall rate of CH<sub>4</sub> formation is difficult to quantify because the total amount of available catalyst surface is unknown (Kress & Tielens 2001). On the other hand, since homogeneous gas-phase chemistry predicts that CO is the dominant carbon species in the solar nebula (Mousis et al. 2002), an increase in the concentration of metallic grains in the zone of giant planet formation, resulting from the outward transit of a dust ring, could lead to an efficient production of CH<sub>4</sub>. This fits well with the current composition of Titan’s atmosphere, where CH<sub>4</sub> is the dominant carbon compound.

Moreover, the enrichments of volatiles measured in the atmospheres of Jupiter and Saturn (Owen et al. 1999; Flasar et al. 2005) have recently been interpreted as requiring an over-solar abundance of water in order to facilitate the trapping of volatiles as clathrate hydrates within the planetesimals produced in the outer nebula (Alibert et al. 2005b; Mousis et al. 2006). Such an increase in the water concentration inside the zone of giant planet formation is still poorly understood. Therefore, since Fischer-Tropsch catalysis has also been suggested as an efficient means of producing H<sub>2</sub>O in astrophysical environments (Willacy 2004), an enhancement of the density of metal particles in this region could explain the presence of large amounts of H<sub>2</sub>O.

## 7. Particle rotation

The first idea to apply photophoresis to the behaviour of protoplanetary disks is still only one year old (Krauss & Wurm 2005). Since then, doubts have been raised on a number of occasions as to the general applicability of photophoresis to dust grains if the particles rotate. In order to answer these concerns, we present the following comprehensive summary of arguments that show that the rotation of dust particles which would be expected in a protoplanetary disk does not prevent their photophoretic drift described above. In previous work, some of these arguments have been mentioned in passing (Krauss & Wurm 2005; Wurm & Krauss 2006), but this is the first time that they have been covered in detail.

The most important point to keep in mind in this context is that we deal with a gaseous disk where any motion of small particles, both linear and rotational, is quickly damped. This behaviour stands in stark contrast to that of the particles in the current Solar system, which retain any rotation for a long period of time. In general, to prevent photophoretic drift, the particles must fulfill both of the following criteria:

- the rotation must be such that the illuminated rotates into shadow, and the shaded side into sunlight; and
- the rotation period of a particle must be shorter than the time taken to reorientate the temperature gradient across its surface.

The timescale for thermal relaxation is established by the conduction of heat through the particle, the thermal emission from the particle surface, and the transfer of heat to colliding gas molecules. Which of these modes dominates the system depends on the particle size and on its thermal properties, the temperature, and the gas density. However, it is important to note that all this becomes unimportant if the rotation axis is oriented in radial direction, lying parallel to the direction of incident radiation. In that case, the temperature gradient will be fixed in space, and photophoresis can act undisturbed, independent of the rotation speed.

Dust particles achieve thermal rotation rates of  $\omega_T = (2kT/I_p)^{1/2}$  (where  $I_p$  is the particle's moment of inertia), around a randomly oriented axis. Krauss & Wurm (2005) showed that this rotation rate is significantly slower than the thermal relaxation timescale from heat conduction, for typical particle properties. By following the same formalism as Krauss & Wurm (2005), it can be estimated that, for the particle sizes and thermal conductivities considered here, the thermal relaxation time due to heat conduction is one to four orders of magnitude shorter than the time constant, for a thermally induced  $180^\circ$  rotation.

Collisions between dust particles will excite rotations about arbitrary axes. To examine the effect of particle-particle collisions, we compare the mean time span between two collisions experienced by a particle with the stopping time  $\tau$  as defined in Eq. (8), which we assume to be of the same order of magnitude as the rotational stopping time. The similarity might be based on the following analogy. A very large but thin plate moving through a viscous medium with the thin section ahead will be decelerated by the frictional interaction between the two sides and the medium (often used to define viscosity). If the plate is bent to form a hollow cylinder, and made to rotate, it is the same interaction on the outside and inside of the cylinder which decelerates the rotation. Thus, the translational motion of the plate and the rotational motion of the cylinder are stopped on the same timescale. In detail, the exact ratio between the stopping time for rotation and for linear motion depends on the morphology of the

particle of interest. However, the coupling mechanisms are the same, and for simplicity we estimate the stopping time for rotation according to Eq. (8). The collision time is given by

$$\tau_{\text{coll}} = (n_p v \sigma_{\text{coll}})^{-1} \quad (15)$$

where  $n_p$  is the particle number density,  $v$  is the relative velocity of the colliding particles, and  $\sigma_{\text{coll}}$  is their collisional cross section. For the particle number density  $n_p$ , we assume a dust to gas mass ratio of 1%, and that all of the mass is contained in particles of radius  $a$ , which gives

$$\tau_{\text{coll}} = 33 \frac{\rho_p a^3}{\rho_g v} \quad (16)$$

The ratio of the two time constants for collisions and coupling is then

$$\frac{\tau_{\text{coll}}}{\tau} = \frac{150\eta}{\rho_g v a C_c} \quad (17)$$

For all relevant combinations of parameters, this ratio is much larger than 1. A population of 1 cm particles, for instance, with a density of 1 g/cm<sup>3</sup> at 1 AU in a 0.2 Myr old disk yields  $\tau_{\text{coll}}/\tau = 1.23 \times 10^6$ , assuming a relative velocity of  $v = 1 \text{ m s}^{-1}$  between the individual particles. If all particles were  $a = 1 \mu\text{m}$  in size, the collision velocities would be solely thermal, on the order of mm/s, and  $\tau_{\text{coll}}/\tau = 1.23 \times 10^3$ . This means that collisions are rather rare events compared to the stopping time, and rotations induced by collisions are therefore damped very quickly. This remains valid as the dust to gas ratio at the midplane of the disk is increased, until the dust-to-gas mass ratio approaches unity, at which point dust motion begins to dominate the disk dynamics. It is therefore clear that collisions are not an obstacle to photophoretic motion.

Irregularly shaped dust particles can also be subject to torques induced by gas drag, by interaction with incident radiation, such as radiation pressure, or by the effect of photophoresis itself. Rotations are induced whenever one or more of these external forces is not in line with the center of mass of a dust grain. All these effects, however, cause rotations around axes aligned radially in a protoplanetary disk, as we will outline here, and can therefore be shown to not affect the photophoretic drift. Weidenschilling (1977, 1997) showed that, in the mid-plane of a gaseous protoplanetary disk, dust particles with gas grain coupling times smaller than their orbital period do *not* have considerable velocities relative to the gas in the direction of their orbital motion, but rather corotate with the gas on a sub-Keplerian orbit. A significant transverse drift motion relative to the gas only occurs for bodies much larger than those we consider. In the radial direction, however, small particles can attain considerable velocities relative to the gas, depending on the interplay of the radial forces at work (described above). Irregularly shaped dust particles that move through a gaseous environment typically show continuous rotation but only around an axis parallel to the direction of their motion relative to the gas. They are aligned along the direction of their motion relative to the gas. This was observed in sedimentation experiments with dust aggregates by Wurm & Blum (2000) for large Knudsen numbers  $Kn = 2 \dots 20$ . This can be understood by the simple geometric reasoning that, at large Knudsen numbers, free molecules impinging upon a particle surface from one side will exert a torque only until the center of particle cross section and the center of mass are aligned along the line of gas-particle motion. It should be pointed out that a high number of gas molecules is needed to set a particle in

rotation. So any effects due to fluctuations of the molecule impacts are statistically washed out. Brenner (1963) also showed theoretically that in the Stokes regime, at small Knudsen numbers, the rotation axis of an arbitrary body moving through a gas will lie parallel to the direction of its translational motion due to the torques exerted upon it by the gas.

The effect of rotation alignment due to incident radiation was investigated experimentally by Abbas et al. (2004). They illuminated nonspherical SiC particles of a few microns diameter which were levitated in an electrodynamic trap with a laser beam and, thereby, forced them into a stable rotational state around an axis parallel to the incident laser beam. In a protoplanetary disk, this would correspond to the radial alignment of rotation axes of those dust grains which are small enough to be efficiently influenced by radiative forces.

Thus, we can conclude that, in general, the rotations of the dust particles (smaller than 10  $\mu\text{m}$ ) in a protoplanetary disk are either too slow, or have rotation axes aligned in such a way that particle rotation is not an obstacle to photophoresis. However, even unfavourable rotation (such as that of larger bodies or of smaller particles in the short time after a collision) will not completely undo photophoresis. We plan experimental studies to investigate the effect of particle rotation on the efficiency of photophoresis in the near future.

## 8. Caveats and future work

There are some aspects of our model which are simplified and need to be treated in more detail in the future. The most important is the size distribution of particles in the disk, with particular emphasis on the smallest particle size that is abundant enough to produce a high opacity. While we believe that our choice of Eq. (13) for the minimum particle size evolution is reasonable, other evolutions can drastically change the motion of the dusty edge, delaying, or speeding up, every part of the evolution. The calculations assume that the dust can be treated as a trace particle with respect to the gas. As a strong density enhancement results at the edge, this assumption might no longer be valid. If the dust density becomes comparable to, or larger than, the gas density, the drift dynamics will change. The dust will move on paths which ever more closely resemble Keplerian orbits, and will carry the gas along with it. The inward drift will get smaller. This is not important for the consideration of the initial inner clearing, but the equilibrium points will shift outwards and the edge might therefore stop its outward motion much further out. However, as a strong particle concentration influences the formation of planetesimals and planets, this is an interesting avenue for further work. Turbulent diffusion might act to smear out the dust distribution at the equilibrium positions in an optically thin disk. It has pronounced influence on the formation and size of the central clearing of the disk. A more rigorous treatment of turbulent diffusion is needed. Also, we describe an optically thin disk with an optically thick model. For the calculation of the behaviour of the outer part of the disk, and the drift of the edge itself, this might be justified, but the disk will change after a gap is cleared. This will not, however, change the principal mechanisms of photophoretic drift. Certainly, the clearing of gaps by planets is entirely possible, and might influence the progression of the initial clearing phase. It should also be noted that our model does not take into account the attenuation of the stellar radiation due to Rayleigh scattering by the gas molecules in the disk, which might reduce the radial drift velocities and, thus, change the positions of the inner disk edge and the equilibrium points. However, the inner holes of transition disks are

currently modelled best as being transparent (Calvet et al. 2002; Forrest et al. 2004; D'Alessio et al. 2005; Bergin et al. 2004; Calvet et al. 2005). For such systems extinction will be only of minor concern for photophoretic effects at the edge.

A lot of unknown properties of the particles with respect to photophoresis are currently hidden in the factor  $J_1$  in Eq. (1). This concerns both the optical properties of grains and heat transfer. It should also be mentioned that particles can experience negative photophoresis, which means that particles can be attracted by light. However, this is restricted to the smallest particles, roughly below 10  $\mu\text{m}$  in size (Mackowski 1989; Rohatschek 1985). The fraction of the disk made up of such small particles (which exhibit either negative photophoresis or no photophoresis) might delay the clearing of the disk until larger particles have grown. However, the drift of the edge is slow for particles smaller than 10  $\mu\text{m}$ , and this will also not change the principle of photophoretic clearing. A better understanding of the thermal conductivity of large dust aggregates is also needed. With respect to the possible applications mentioned in Sect. 6 it should be pointed out that we do not know the precise point in time at which the photophoretic sweep of dust described in this paper starts. The aspect of the chronological relation of the photophoretic dust migration to other events and epochs in the evolution of the Solar nebula should be addressed in future studies. Despite these apparent limitations, and the number of parameters which are still poorly defined or unknown, we regard photophoretic clearing as a mechanism that is very likely to be important in the formation of both our Solar system, and those around other stars.

*Acknowledgements.* O. Krauss and G. Wurm are funded by the Deutsche Forschungsgemeinschaft, and Jonti Horner acknowledges the support of the Swiss National Science Foundation.

## References

- Abbas, M. M., Craven, P. D., Spann, J. F., et al. 2004, *ApJ*, 614, 781  
 Alexander, D. R., & Ferguson, J. W. 1994, *ApJ*, 437, 879  
 Alibert, Y., Mordasini, C., Benz, W., & Winisdoerffer, C. 2005a, *A&A*, 434, 343  
 Alibert, Y., Mousis, O., & Benz, W. 2005b, *ApJ*, 622, L145  
 Alibert, Y., Mousis, O., Mordasini, C., & Benz, W. 2005c, *ApJ*, 626, L57  
 Alibert, Y., Mousis, O., & Benz, W. 2005d, *A&A*, 439, 1205  
 Bell, K. R., & Lin, D. N. C. 1994, *ApJ*, 427, 987  
 Bich, E., Millat, J., & Vogel, E. 1990, *J. Phys. Chem. Ref. Data*, 19, 1289  
 Blum, J., & Wurm, G. 2000, *Icarus*, 143, 138  
 Blum, J., Wurm, G., Kempf, S., & Henning, Th. 1996, *Icarus*, 124, 441  
 Blum, J., Wurm, G., Kempf, S., et al. 2000, *Phys. Rev. Lett.*, 85, 2426  
 Beresnev, S., Chernyak, V., & Fomyagin, G. 1993, *Phys. Fluids A*, 5, 2043  
 Bergin, E., Calvet, N., Sitko, M. L., et al. 2004, *ApJ*, 614, L133  
 Bouvier, J., Alencar, S. H. P., Harries, T. J., Johns-Krull, C. M., & Romanova, M. M. 2006, in *Protostars and Planets V*, ed. B. Reipurth, D. Jewitt, & K. Keil (Tucson: University of Arizona Press), in press  
 Bouwman, J., de Koter, A., Dominik, C., et al. 2003, *A&A*, 401, 577  
 Brenner, H. 1963, *Chem. Eng. Sci.*, 18, 1  
 Calvet, N., D'Alessio, P., Hartmann, L., et al. 2002, *ApJ*, 568, 1008  
 Calvet, N., D'Alessio, P., Watson, D. M., et al. 2005, *ApJ*, 630, L185  
 Campins, H., & Ryan, E. V. 1989, *ApJ*, 341, 1059  
 Cheremisin, A. A., Vassilyev, Y. V., & Horvath, H. 2005, *Aerosol Sci.*, 36, 1277  
 Čuk, M., & Gladman, B. J. 2006, *Icarus*, 183, 362  
 Cunningham, E. 1910, *Proc. Roy. Soc.*, 83, 357  
 D'Alessio, P., Hartmann, L., Calvet, N., et al. 2005, *ApJ*, 621, 461  
 Dominik, C., Blum, J., Cuzzi, J., & Wurm, G. 2006, in *Protostars and Planets V*, ed. B. Reipurth, D. Jewitt, & K. Keil (Tucson: University of Arizona Press), in press  
 Dullemond, C. P., & Dominik, C. 2004, *A&A*, 421, 1075  
 Ehrenhaft, F. 1918, *Ann. Phys.*, 56, 81  
 Flasar, F. M., Achterberg, R. K., Conrath, B. J., et al. 2005, *Science*, 307, 1247  
 Forrest, W. J., Sargent, B., Furlan, E., et al. 2004, *ApJS*, 154, 443  
 Greaves, J., Fischer, D. A., & Wyatt, M. C. 2006, *MNRAS*, 366, 283  
 Hayashi, C., Nakazawa, K., & Nakagawa, Y. 1985, in *Protostars and Planets II*, ed. D. C. Black, & M. S. Matthews (Tucson: University of Arizona Press), 1100

- Hettner, G. 1928, *Ergebn. Exakt. Naturwiss.*, 7, 209
- Horner, J., Mousis, O., & Hersant, F. 2006, *Earth Moon and Planets*, 4
- Hutchins, D. K., Harper, M. H., & Felder, R. L. 1995, *Aerosol Sci. Tech.*, 22, 1995
- Ida, S., Larwood, J., & Burkert, A. 2000, *ApJ*, 528, 351
- Incropera, F. P., & DeWitt, D. P. 2002, *Heat and Mass Transfer* (John Wiley & Sons)
- Jewitt, D., & Sheppard, S. 2005, *Space Sci. Rev.*, 116, 441
- Kenyon, S. J., & Bromley, B. C. 2004, *Nature*, 432, 598
- Krauss, O., & Wurm, G. 2005, *ApJ*, 630, 1088
- Kress, M. E., & Tielens, A. G. G. M. 2001, *Meteor. Planet. Sci.*, 36, 75
- Mackowski, D. W. 1989, *Int. J. Heat Mass Transfer*, 32, 843
- Mousis, O., & Alibert, Y. 2006, *A&A*, 448, 771
- Mousis, O., Gautier, D., & Bockelée-Morvan, D. 2002, *Icarus*, 156, 162
- Najita, J. R., Carr, J. S., Glassgold, A. E., & Valenti, J. A. 2006, in *Protostars and Planets V*, ed. B. Reipurth, D. Jewitt, & K. Keil (Tucson: University of Arizona Press), in press
- Owen, T. C., Mahaffy, P. R., Niemann, H. B., et al. 1999, *Nature*, 402, 269
- Papaloizou, J., & Terquem, C. 1999, *ApJ*, 521, 823
- Paraskov, G., Wurm, G., & Krauss, O. 2006, *ApJ*, 648, 1219
- Petit, J.-M., Mousis, O., Alibert, Y., & Horner, J. 2006, *Lunar Planet. Sci.*, 37, 1558
- Presley, M. A., & Christensen, P. R. 1997, *J. Geophys. Res.*, 102, 6535
- Prinn, R. G., & Fegley Jr., B. 1989, in *Origin and Evolution of Planetary and Satellites Atmospheres*, ed. S. K. Atreya, J. B. Pollack, & M. S. Matthews (Tucson: University of Arizona Press), 78
- Rettig, T. W., Haywood, J., Simon, T., Brittain, S. D., & Gibb, E. 2004, *ApJ*, 616, L163
- Rohatschek, H. 1985, *J. Aerosol Sci.*, 16, 29
- Rohatschek, H. 1995, *J. Aerosol Sci.*, 26, 717
- Saumon, D., Chabrier, G., & van Horn, H. M. 1995, *ApJS*, 99, 713
- Sekine, Y., Sugita, S., Shido, T., et al. 2005, *Icarus*, 178, 154
- Shakura, N. I., & Sunyaev, R. A. 1973, *A&A*, 24, 337
- Sicilia-Aguilar, A., Hartmann, L., Calvet, N., et al. 2006, *ApJ*, 638, 897
- Sitko, M. L., Lynch, D. K., Russell, R. W., et al. 2004, *ApJ*, 612, 576
- Supulver, K. D., & Lin, D. N. C. 2000, *Icarus*, 146, 525
- Veras, D., & Armitage, P. J. 2004, *MNRAS*, 347, 613
- Weidenschilling, S. J. 1977, *MNRAS*, 180, 57
- Weidenschilling, S. J. 1997, *Icarus*, 127, 290
- Weidenschilling, S. J. 2000, *Space Sci. Rev.*, 92, 281
- Willacy, K. 2004, *ApJ*, 600, 87
- Wurm, G., & Blum, J. 2000, *ApJ*, 529, L57
- Wurm, G., & Krauss, O. 2006, *Icarus*, 180, 487
- Wurm, G., Paraskov, G., & Krauss, O. 2005, *Icarus*, 178, 253